



P2C-05: PREDICTION OF FILM FRACTION IN AN ANNULAR GAS-LIQUID FLOW ACROSS A VERTICAL LARGE DIAMETER PIPE

A. M. Badeko^{1,*}, A. Mohammed¹, A. Mukhtar¹, J. N. Samson²

¹Chemical Engineering Department Federal University of Technology, Minna, Niger State, P. M. B. 65, Nigeria.

²Chemical Engineering Department University of Abuja, Nigeria

Corresponding author: Email: mabadeko@gmail.com, Tel: +2348036528250

Abstract

Several research efforts were made in the past to study annular flow for both vertical and horizontal pipes, but the attention was mainly on small diameter pipes (diameter less than 100mm) with little or no emphasis laid on large diameter pipes. However, in this research work an attempt is made to develop an empirical model that can predict liquid film fraction across a vertical large diameter pipe ($D = 127\text{mm}$). The empirical model was based on some dimensionless numbers such as liquid and gas Reynolds number and also liquid and gas Weber Number. The empirical model developed in this work for the prediction of liquid film fraction is $\epsilon = 1.9 \times 10^7 \text{Re}_G^{-1.4688} \text{Re}_L^{0.0701} \text{We}_G^{-0.2276} \text{We}_L^{-0.0009}$. There was good agreement between the predicted liquid film fraction and the experimental values when measured at different vertical positions across the vertical riser (i.e. 8.1m, 8.3m, 8.4m and 8.5m). Using the Pearson product moment correlation coefficient, the predictions were 90.6%, 84.7%, 81.1% and 98.3% respectively.

Keywords: Dimensionless number; Empirical model; Liquid film fraction; Superficial velocity.

1.0 INTRODUCTION

Annular gas-liquid two phase flow is a very important flow configuration that occurs in many relevant applications such as in nuclear reactors, power plants, petroleum and process industries. It is a flow regime that is characterized by a high velocity gas flowing within the core of the pipe carrying some entrained liquid droplets and a thin liquid layer stationary positioned and/or moving along the internal wall of the pipe (Kaji and Azzopadi, 2010). Typically, annular gas-liquid flow are usually encountered in heat exchangers, deepwater risers in hydrocarbon production, gas condensates transport pipes, air conditioners and steam boilers used in nuclear and thermal power plants. Accurate prediction of the flow behaviour such as film fraction is very important for the safe and efficient design of heat transfer equipment, oil and gas

pipelines and other process transport equipment.

Several research works have been done in the past decades on upward and downward two-phase air-water annular flow using smaller diameter pipes (i.e diameter less than 100mm) and a lot of mechanistic and empirical models have been developed to characterize the flow behaviour, however for large diameter pipes (i.e diameter greater than 100mm) not much research effort have been made as compared to the former leading to dearth of information in the literature for large diameter pipes. Consequently, data and models for small diameter pipes have been extrapolated for use in the design and operation involving large diameter pipes (Abdulkadir et al., 2019) which in most cases do not yield accurate results. However, it has been observed by other researchers such as Omebere-Iyari (2006), Kaji and Azzopadi

(2010), Aliyu (2015), Lao et al. (2012) among others that the flow structures in large diameter pipes are different when compared to the small diameter pipes for instance the conventional slug flow characterised by bullet shaped Taylor bubbles does not manifest in large diameter pipes instead, there is a gradual transition from bubbly to churn flow (Aliyu, 2015).

Meanwhile, an attempt is made in this research work to develop an empirical model to predict film fraction in an annular air-water flow across a vertical large diameter pipe. The film fraction is a very important hydrodynamic parameter and is useful in determining the pressure drop and in the design of separation equipment in the petroleum industry (Ternyik et al, 1995). The models and empirical correlations that currently exist in open literature used in predicting film fraction were developed using data from small diameter pipes and cannot be applied correctly in the design of systems involving large diameter pipes such as risers used in petroleum production. There is therefore the need to develop a new film fraction correlation based on data from large diameter pipes and this forms the gap that this research effort tries to address.

2. METHODOLOGY

In this research, a systematic procedure for developing an empirical dynamic model as proposed by Ljung, (1999) was used. The procedure consists of the following steps:

2.1 Formulation of model objectives

The primary objective of the empirical model to be developed is for the model to be able to predict liquid film fraction in an annular flow across a vertical large diameter pipe (127mm) using the superficial velocity, density, viscosity and surface tension of both the air and water as the input parameters. However, these input

parameters were used to determine the Weber number and the Reynolds number for both phases and these dimensionless numbers were used in the model formulation.

2.2 Selection of the input and output variables for the model

The experimental data used in this research work were obtained from the work performed by Abdulkadir, (2011) at the L3 Laboratories of the Department of Chemical and Environmental Engineering at the University of Nottingham. The experiments were performed using the 127mm diameter riser where the film fraction measurements were carried out at positions 8.1m, 8.3m and 8.4m respectively along the vertical direction. Abdulkadir, (2011) reported in his work that the temperature of the air and the mains tap water were all maintained at 25°C.

2.3 Evaluation of available data

The experimental data obtained from the work of Abdulkadir (2011) where measurements of film fraction were done at different combination of gas and liquid superficial velocities was analysed using the Microsoft excel. In the analysis, the Weber Number and the Reynolds Number for both the liquid phase (water) and the gas phase (air) were computed. The physical properties of the phases were obtained at the experimental conditions of 25°C temperature and pressure of 2.0 bar. The density of air and that of water are 3.53kg/m³ and 986kg/m³ respectively. The surface tension was also obtained as 0.07199 N/m and the viscosity of air at 25°C is 8.90 x 10⁻⁴ Pa.s. The gas Weber number was computed using equation (1) as stated below:

$$Weg = \frac{\rho_g u_{gD}^2}{\sigma} \left(\frac{\Delta\rho}{\rho_g} \right)^{\frac{1}{4}} \quad (1)$$

But the liquid Weber Number was computed using the equation below:

$$We_L = \frac{\rho_l u_l^2 D}{\sigma} \quad (2)$$

The liquid and gas Reynolds Number will be computed using the equation below:

$$Re = \frac{\rho u D}{\mu} \quad (3)$$

Where ρ = Density, kg / m³ (subscript 'g' and 'l' for both gas and liquid respectively)

U = superficial velocity, m/s (subscript 'g' and 'l' for both gas and liquid respectively)

D = Pipe diameter, m

σ = Surface tension, N/m

μ = Viscosity, Ns/m²

The plot of the film fraction with each of these dimensionless numbers will be made using the power law to determine the functional relationship between them.

$$\varepsilon = (We_g)^a \quad (4)$$

$$\varepsilon = (We_l)^b \quad (5)$$

$$\varepsilon = (Re_g)^c \quad (6)$$

$$\varepsilon = (Re_l)^d \quad (7)$$

where ε is the film fraction, We_g , We_l , Re_g and Re_l are the Weber Number and the Reynolds Number for both the gas and liquid phase. The exponents a, b, c, and d are determined graphically when the plot of these dimensionless numbers are made with the film fraction. The exponents from the equations were entered into a Microsoft Excel program called SOLVER as the initial values for iteration. The SOLVER is a Microsoft Excel add-in program used for 'what if' analysis. It is used to find an optimal (maximum or minimum) value for a formula in one cell called the objective cell subject to constraints or limits, on the values of other formula cells on a worksheet. SOLVER works with a group of cells, called

decision variables or simply variable cells that are used in computing the formulas in the objective and constraint cells. SOLVER adjusts the values in the decision variable cells to satisfy the limits on constraint cells and produce the result you want for the objective cell. In this work, the exponents on each of the dimensionless numbers are the decision variables, the formula is the empirical model consisting of the gas and liquid Weber number and the gas and liquid Reynolds number to predict film fraction while the constraint cell is the sum of the squares of the difference between the experimental and predicted film fraction. The goal is to minimise the constraint cell as much as possible in order to improve the predictive ability of the empirical correlation.

2.4 Selection of the model structure and level of model complexity

Based on the description of the physics of the system adequately represented by the Weber Number and the Reynolds Number for the gas and liquid phases, the functional form of the empirical model to predict film fraction across a vertical pipe in an annular flow can be obtained as:

$$\varepsilon = (We_g)^a (We_l)^b (Re_g)^c (Re_l)^d \quad (8)$$

The proposed empirical model is a simple model to use because the input parameters (the superficial velocities for both the gas and liquid phase and their physical properties) can easily be obtained from laboratory measurements.

3. RESULTS AND DISCUSSION

3.1 Dependence of liquid film fraction on the gas superficial velocity at constant liquid superficial velocity

From the Figure 1, it can be observed that as the superficial velocity of the gas increases from 950m/s to 1,500m/s while keeping the superficial velocity of the liquid constant (40m/s), the liquid film fraction which is essentially the fraction of the liquid in the riser existing as a thin film

layer along the internal wall of the riser decreases from 0.06857 to 0.03382 along the 8.1m measuring position in the vertical riser and the same applies to other measuring locations in the riser. The reduction of the film fraction at constant superficial liquid velocity and increasing gas velocity is as a result of the increasing inertia force created as a result of increasing superficial velocity which potentially peels off a portion of the liquid film along the interface between the film layer and the gas core thereby increasing the amount the liquid entrained in the gas core while reducing the liquid film fraction as alluded to by other researchers such as Thome and Cioncolini (2009).

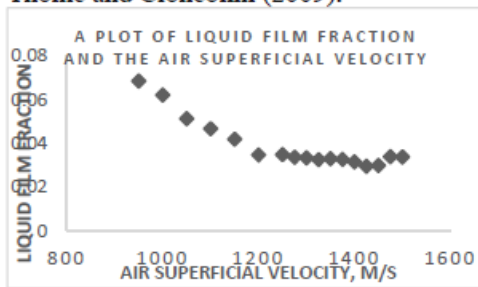


Figure 1: Gas superficial velocity versus liquid film fraction at constant superficial liquid velocity.

3.2 Dependence of the liquid film fraction on the liquid superficial velocity.

From Figure 2, it can be observed that as the superficial liquid velocity increases from 40m/s to 150m/s and at constant superficial gas velocity, the liquid film fraction increases from 0.039103 to 0.060516 though the film fraction remained almost constant between 60m/s and 150m/s superficial liquid velocity. The increase in the liquid film fraction as the superficial liquid velocity increases is as a result of the increased amount of liquid available within the measuring location which essentially increases as the superficial liquid velocity increases.

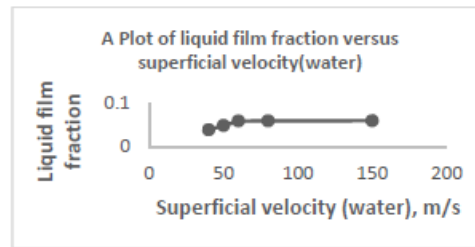


Figure 2: Liquid superficial velocity versus liquid film fraction at constant superficial gas velocity.

3.3 Dependence of the liquid film fraction on the gas Reynolds number (Rec)

Figure 3 shows the plot of the liquid film fraction and the gas Reynolds Number. In order to understand the variation of the liquid film fraction as the fluid velocity increases, there is a need to understand the nature of forces at play in forming the liquid film thickness and entrained droplets within the gas core. Some of the forces include the inertia force and the viscous force. The competition between these forces determines the amount of liquid that will form the thin liquid film and equally the liquid that will be entrained into the gas core. The dimensionless number that captures the interplay between these forces is the Reynolds Number. In the Figure 4.3 above, it can be observed that as the gas Reynolds Number increases from 478,533 to 755,578 which implies a highly turbulent flow regime, the liquid film fraction decreases from 0.068568 to 0.03382. The decrease in the liquid film fraction as gas Reynold number increases is a result of the increase in the inertia force which tend to convert some layer of the liquid film into droplets in the gas core, thereby reducing its thickness and invariable the overall liquid film fraction (Berna et al, 2014).

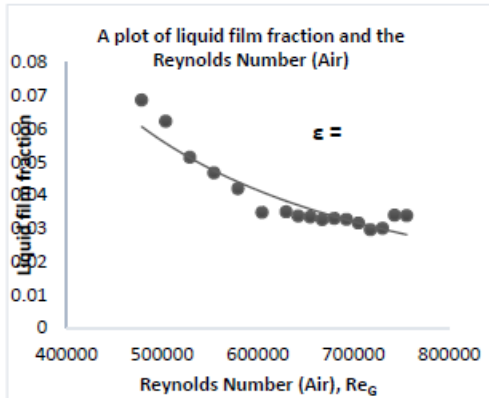


Figure 3: Liquid film fraction versus the Gas Reynolds Number.

2.4 Dependence of the liquid film fraction on the liquid Reynolds number (Re_L)

Figure 4 shows the relationship between the liquid film fraction and the liquid Reynolds Number. From the chart, it can be observed that the liquid film fraction increases from 0.039103 to 0.060516 as the liquid Reynolds Number increases from 5,627,955 to 21,104,831. The increase in the liquid film fraction as the liquid Reynolds Number increases is as a result of the increase in the superficial velocity of the liquid which tends to increase the quantity of the liquid moving into the measuring location thereby increasing the thickness of the liquid film around the internal wall of the riser and inadvertently increasing the liquid film fraction.

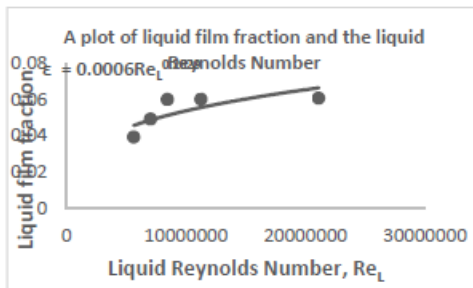


Figure 4: Liquid film fraction versus the Liquid Reynolds Number.

3.5 Dependence of the liquid film fraction on the gas Weber number (We_G)

Figure 5 shows the relationship between the liquid film fraction and the gas Weber Number. The Weber Number is the dimension number that captures the interplay of inertia force and surface tension force which according to Ju (2015) governs the formation of the liquid film thickness. In fact, according to Ju (2015), the inertia force tends to break the liquid at the interface (i.e. to form droplets) while the surface tension force tends to keep the liquid at the interface (i.e. thin liquid film thickness). From Figure 5, it can be observed that as the gas Weber Number increases from 5,600,101 to 13,961,470, the liquid film fraction decreases from 0.068568 to 0.03382. The decrease in the liquid film fraction as the gas Weber Number increases is as a result of the increase in the inertia force which tends to break the thin liquid layer into tiny droplets thereby reducing the thickness of the thin liquid film and the overall reduction of the liquid film fraction.

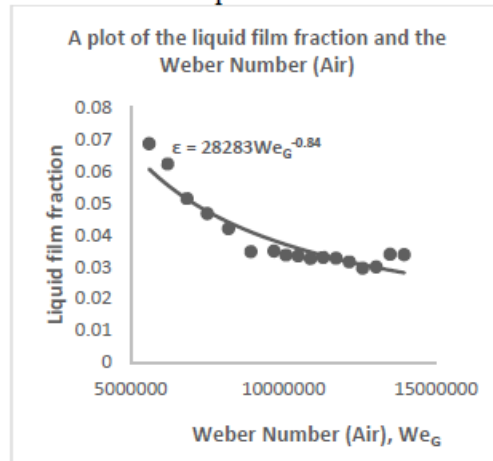


Figure 5: Liquid film fraction versus the Gas Weber Number

3.5 Dependence of the liquid film fraction on the liquid Weber number (We_L)

Figure 6 shows the relationship between the liquid film fraction and the Liquid Weber Number. From the chart, it can be

observed that as the liquid Weber Number increases from 2783098 to 39137311, the liquid film fraction equally increases from 0.039103 to 0.060516. The increase in the liquid film fraction as the liquid Weber Number increases is as a result of the increase in the superficial velocity of the liquid which tends to move a large quantity of the liquid and at constant gas superficial velocity, increases the thickness of the liquid film along the internal wall of the riser thereby increasing the film fraction.

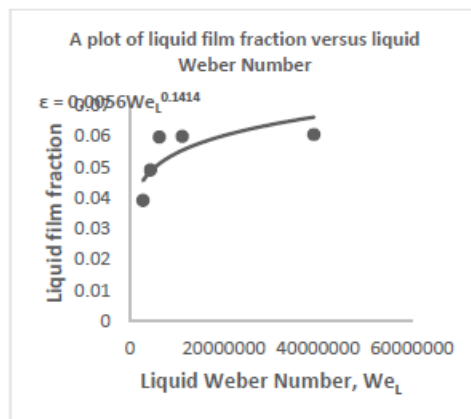


Figure 4.6: Liquid film fraction versus the Liquid Weber Number.

The overall relationship between the liquid film fraction and the various dimensionless numbers can be summarized below:

For the gas Reynolds Number:

$$\epsilon = 2 \times 10^8 \text{Re}_G^{-1.68} \quad (1)$$

For the liquid Reynolds Number:

$$\epsilon = 0.0006 \text{Re}_L^{0.2829} \quad (2)$$

For the gas Weber Number:

$$\epsilon = 28283 \text{We}_G^{-0.84} \quad (3)$$

For the liquid Weber Number:

$$\epsilon = 0.0056 \text{We}_L^{0.1414} \quad (4)$$

On combining all the dimensionless numbers to determine the overall relationship between them and the liquid film fraction, we have:

$$\epsilon = 1.9 \times 10^7 \text{Re}_G^{-1.68} \text{Re}_L^{0.2829} \text{We}_G^{-0.84} \text{We}_L^{0.1414} \quad (5)$$

The final correlation for the liquid film model can be represented as:

$$\epsilon = 1.9 \times 10^7 \text{Re}_G^{-1.4688} \text{Re}_L^{0.0701} \text{We}_G^{-0.2276} \text{We}_L^{-0.0099}$$

4.0 CONCLUSION

In this research work, the relationship between the liquid film fraction and the superficial gas and liquid velocities was investigated. It was observed that the liquid film fraction decreases as gas superficial velocity increases while it increases as the liquid superficial velocity increases. Similarly, the relationship between the liquid film fraction and the various dimensionless numbers that adequately describe the physics of the system were investigated. The dimensionless numbers include the gas and liquid Reynolds Number and gas and liquid Weber Number. It was observed that as the gas Reynolds Number and gas Weber Number increases, the liquid film fraction decreases and the reverse occur when the liquid Reynolds and Weber Numbers increases. Based on the relationships between these dimensionless numbers and the liquid film fraction, a new correlation that can predict liquid film fraction was developed, i.e. $\epsilon = 1.9 \times 10^7 \text{Re}_G^{-1.4688} \text{Re}_L^{0.0701} \text{We}_G^{-0.2276} \text{We}_L^{-0.0099}$.

REFERENCES

- Aliyu, A.M., (2015). Vertical Annular Gas-Liquid Two-phase Flow in Large diameter Pipes. A PhD dissertation. Cranfield University, United Kingdom.
- Aziz, K., Govier, G.W. & Forgasi, M., 1972. Pressure Drop In Wells Producing Oil And Gas. *Journal of Canadian Petroleum Technology*, 11(03).
- Abdulkadir, M. (2011). Experimental and computational fluid dynamics (CFD) of gas-liquid flow in bends. PhD thesis,

University of Nottingham, United Kingdom.

Abdulkadir M., U.P. Mbalisigwe A. D. Zhao b, V. Hernandez-Perez c, B.J. Azzopardi d, S. Tahir e Characteristics of churn and annular flows in a large diameter vertical riser International Journal of Multiphase Flow, 36(4), 303–313. Bhagwat, S.M., Mollamahmutoglu, M. & Ghajar, A.J., (2012). Experimental investigation and performance evaluation of isothermal frictional two phase pressure drop correlations in vertical downward gas-liquid two phase flow. In *Proceedings of the ASME 2012 Summer Heat Transfer Conference*. Rio Grande, Puerto Rico: ASME, 1–12.

Bhagwat, S.M., Mollamahmutoglu, M. & Ghajar, A.J., 2012. Experimental investigation and empirical analysis of non-boiling gas-liquid two-phase heat transfer in vertical downward pipe orientation. In Rio Grande, Puerto Rico: *ASME*, 1–11.

Bhagwat, S.M. & Ghajar, A.J., 2012. Similarities and differences in the flow patterns and void fraction in vertical upward and downward two phase flow. *Experimental Thermal and Fluid Science*, 39, 213–227.

Chen, L., (2006). Flow patterns in upward two-phase flow in small diameter tubes. PhD thesis, Brunel University UK.

Dalkilic, A. S., Laohalertdecha, S. & Wongwises, S., 2008. Two-phase friction factor in vertical downward flow in high mass flux region of refrigerant HFC-134a during condensation. *International Communications in Heat and Mass Transfer*, 35(9), 1147–1152.

Duns, H. & Ros, N.C.J., 1963. Vertical flow of gas and liquid mixtures in wells. In *World Petroleum Congress*. Frankfurt, Germany: World Petroleum Congress.

Hagedorn, A. & Brown, K.E., 1965. Experimental Study of Pressure Gradients Occurring During Continuous Two-Phase Flow in Small-Diameter Vertical Conduits. *Journal of Petroleum Technology*, 17(4), 475 – 484.

Kaji, R. & Azzopardi, B.J., (2010). The effect of pipe diameter on the structure of gas/liquid flow in vertical pipes. *International Journal of Multiphase Flow*, 36(4), 303–313.

Lao, L., Xing, L. & Yeung, H., (2012). Behaviours of elongated bubbles in a large diameter riser. In *Multiphase 8*. Banff, Canada: BHR Group, 381–392.

Oddie, G., Shi, H., Durlafsky, L.J., Aziz, K., Pfeffer, B., & Holmes, J.A., (2003). Experimental study of two and three phase flows in large diameter inclined pipes. *International Journal of Multiphase flow*, 29, 527 – 588.

Oliemans, R.V.A., Pots, B.F.M. & Trompe, N., 1986. Modelling of annular dispersed two-phase flow in vertical pipes. *International Journal of Multiphase Flow*, 12(5), 711–732.

Omebere-Iyari, N.K., (2006). The effect of pipe diameter and pressure in vertical two-phase flow. University of Nottingham.

Skopich, A. et al., 2015. Pipe-diameter effect on liquid loading in vertical gas wells. *SPE Production and Operations*, 30(2), 164–176.

Tsoukalas, L.H., Ishii, M. & Mi, Y., 1997. A neurofuzzy methodology for impedance-based multiphase flow identification. *Engineering Applications of Artificial Intelligence*, 10(6), 545–555.

Tambouratzis, T. & Pázsit, I., 2010. A general regression artificial neural network for two-phase flow regime identification.

Annals of Nuclear Energy, 37(5), 672–680.

Liu, Y. & Zhang, S., 2010. Local flow regime identification for boiling two-phase flow by BP neural networks approach. In *Sixth International Conference on Natural Computation*. 362–366.

Zhao, X., 2005. *Mechanistic based models for slug flow in vertical pipes*. Texas Tech University.